Journal of Power and Energy Engineering, 2018, 6, 63-85
http://www.scirp.org/journal/jpee
ISSN Online: 2327-5901
ISSN Print: 2327-588X

Technology Readiness of a Vertical-Axis Hydro-Kinetic Turbine

Stefan Runge, Thorsten Stoesser, Emily Morris, Madeleine White

Hydro-Environmental Research Centre, Cardiff University, Cardiff, Wales, UK
Email: stoesser@cf.ac.uk

How to cite this paper: Runge, S., Stoesser, T., Morris, E. and White, M. (2018) Technology Readiness of a Vertical-Axis Hydro-Kinetic Turbine. *Journal of Power and Energy Engineering*, **6**, 63-85.
https://doi.org/10.4236/jpee.2018.68004

Received: April 26, 2018
Accepted: August 26, 2018
Published: August 29, 2018

Abstract

In this paper, the development of a vertical axis hydrokinetic twin turbine for harvesting energy from flowing water in man-made channels is described. The Technology Readiness Level (TRL) assessment procedure, developed by NASA and modified by the US Department of Energy, is followed and it is shown that the hydrokinetic turbine successfully reaches TRL 7, which is a full-scale, similar (prototypical) system demonstrated in a relevant environment. The concept of the twin turbine (TRL 1 - 3) is first validated and tested using a 1:10 scale laboratory model at Cardiff University and efficiencies of up to 75% are achieved (TRL 4 - 5). In order to justify system functionality and performance in a relevant environment as well as up-scalability, a 1:3 scale model of the twin turbine is implemented and tested in a discharge channel of a water treatment plant in Atlanta, thereby achieving TRL6. This paved the way for an application in the form of an array of ten full-scale twin turbine prototypes, including all relevant components such as housing, drive-train, gear-box and generator. Successful deployment and testing in the South Boulder Canal near Denver means that the hydrokinetic twin turbine system reached TRL7.

Keywords

Hydro-Turbine, Vertical-Axis, VAT, Micro-Hydro, TRL, Technology Readiness Level

1. Introduction

Growing energy demand and climate change are main drivers for the fast evolution of novel energy conversion systems. While energy production during the second half of the past century was focused on large-scale fossil or nuclear power plants, the 21st century might be the era of eco-sensitivity, sustainability and the

decentralization of power generation. In other words, many small, "green" generation units can replace a few large, environmentally-questionable plants with the benefit of low capital costs, reduced transformational energy losses and potentially zero carbon emission [1].

Water current turbines, also called hydrokinetic or in-stream turbines, have received growing interest in many parts of the world. Two main areas where hydrokinetic devices can be used for power generation purposes are tidal currents and river streams. These turbines generate power from the kinetic energy of a flowing stream of water without the use of a dam or a barrage and so it consequently does not need to interfere with the natural course of rivers. Water current turbines can be installed in any flow with a velocity greater than 0.5 m/s [2]. Because of low investment requirements and operational costs, hydrokinetic turbines promise to be cost effective in comparison to other technologies. The continuous supply of electrical energy is a big advantage in comparison to solar or wind power.

On the following pages, the successful development of a hydro-kinetic-turbine for harvesting energy from flowing water in man-made channels (such as water-treatment plant effluents, irrigation channels etc.) is described and assessed with help of technology readiness levels (TRL). As shown in **Table 1**, TRL levels range from 1 to 9, and this way of assessing technology maturity was pioneered by the NASA and modified by the US Department of Energy. The purpose of the TRL characterization is to help assess a technology development process and iterate the design with respect to matching technical scope, schedule, costs and safety [3].

2. Hydrokinetic Twin Turbine Technology Concept (TRL 1 - 3)

The aim of the here presented energy conversion systems is to convert the movement of flowing water in a channel into mechanical torque and further, into electricity in the most efficient and sustainable way. Each component of the turbine system has been designed to integrate as a unit and can be split into 5 subsystems as shown in **Figure 1**.

The concrete structure (1-4) comprises four individual parts (a bottom plate, two columns and a bridge) and it serves several purposes: as a structural member to hold the turbine components in place safely and as a gravity base (stays in place due to its self-weight) which makes additional foundation obsolete. In operation, the bridge is not submerged and hosts the power take/off which consists of drive train, gearbox and generator.

The structure hosts a co-rotating vertical axis twin rotor system that is placed between bridge and bottom plate. The rotors are held in place by four bearings (18). Each rotor consists of a stainless-steel shaft (17), three hubs (10), six spokes (12 - 16) and three blades (11) (**Figure 2** LHS). As soon as water flows across the rotors at a certain minimum speed, the airfoil-shaped blades are generating enough lift to start rotating.

Table 1. Technology Readiness Levels from DOE guide, without detailed description [3].

Relative Level of Technology Development	Technology Readiness Level	TRL-Definition
System Operations	TRL 9	Actual system operated over the full range of expected mission conditions.
System Commissioning	TRL 8	Actual system completed and qualified through test and demonstration.
	TRL 7	Full-scale, similar (prototypical) system demonstrated in relevant environment.
Technology Development	TRL 6	Engineering/pilot-scale, similar (prototypical) system validation in relevant environment.
	TRL 5	Laboratory scale, similar system validation in relevant environment.
	TRL 4	Component and/or system validation in laboratory environment.
Research to prove feasibility	TRL 3	Analytical experimental critical function and/or characteristic proof of concept.
Basic technology research	TRL 2	Technology concept and/or application formulated.
	TRL 1	Basic principles observed a reported.

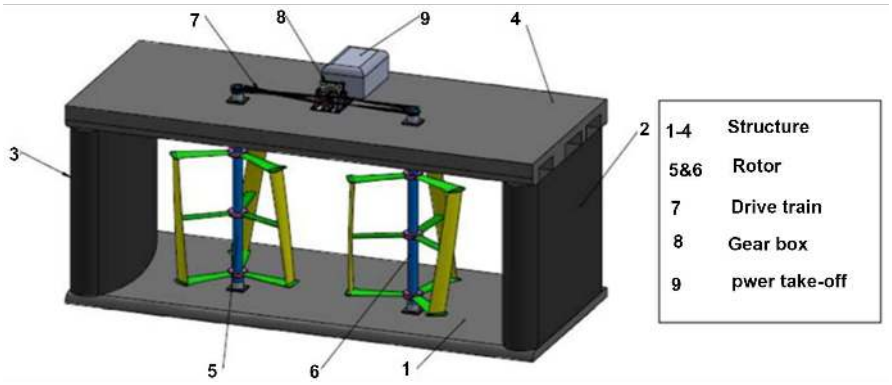

Figure 1. Five subsystems of the hydro-kinetic vertical axis turbine system.

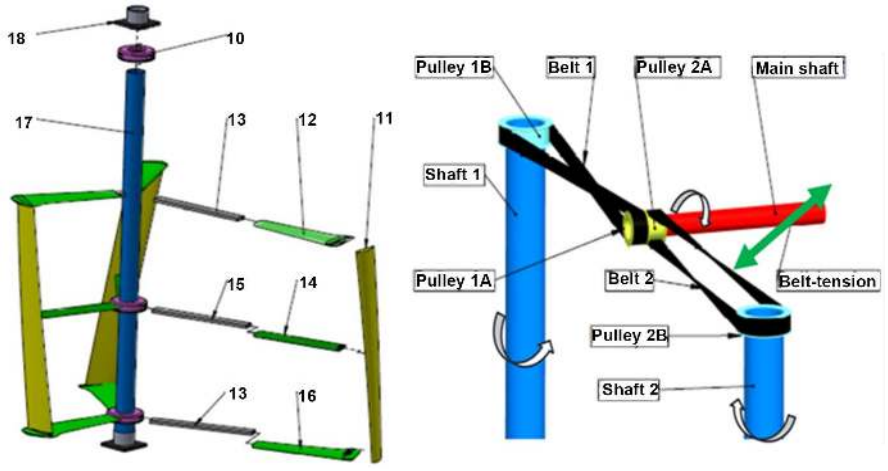

Figure 2. LHS, exploded view of a rotor. RHS, components of drive train.

The rotational movement of the rotor is transferred via the two rotor shafts to a belt drive which consists of two 90˚ twisted timing belts, two large pulleys, two small pulleys and a horizontally orientated main shaft (**Figure 2** RHS). The belt drive enables transferring the torque from the two rotor shafts onto a main drive train shaft and allows a speed or torque adjustment to appreciate gearbox or generator specification. Attached to the main drive train shaft is a gearbox and subsequently an electrical generator which are not a part of this report. A patent of this system was filed in October 2017 [4].

3. Technology Development - Laboratory Testing (TRL 3-5)

Laboratory tests were undertaken in the Hydro-Environmental Research Laboratory at Cardiff University. For testing the turbine, a 17 meters long, 1.2 meters wide and 1 m deep flume was used. For most experiments, the water depth was set to 0.5 m. The water is driven by an axial flow impeller which allows flow speeds of up to 1.5 m/s at the given water depth. The channel sidewalls are made out of glass which allowed visual observations during testing (**Figure 3**).

The rotors were mounted to the bottom of the flume via lubricated stainless steel bearings which were screwed onto a PVC board that was glued to the flume bed. The PVC board had various threaded holes which allowed for different rotor positions. The top of the rotors were held by pillow block bearings which were attached to a movable bridge across the top of the flume allowing a rotor displacement in any direction. Further, the bridge accommodated the PTO consisting of drive train, generator and measurement equipment (**Figure 3** bottom right).

In order to quantify the mechanical output of the twin-rotors, a torque transducer (Futek TRS605) was affixed at center position of the main shaft. Either a disc break or a generator was attached to the other end of the main shaft in order to apply a resistance to the rotors. The measurements of the torque transducer were collimated by a "Lab-Jack U6" and analyzed by "DAQFactory® Express" and "MS-Excel®".

More than 200 individual tests were conducted with the target to study and optimize the rotor, the housing structure and eventually the twin-rotor assembly. In the following, the researched aspects are individually introduced, theoretically explained and the results presented and discussed.

3.1. Experimental Rotor Optimization

In contrast to a straightforward rotor design with very little moving parts, the hydrodynamics of Vertical-Axis Turbine (VATs) are complex due to a constant changing angle of attack and the interaction of vortices [5]. Numerical research shed light on the detailed flow-turbine interaction. Large eddy simulations (LES) [6] [7] and Reynolds averaged Navier-Stokes (RANS) methods [8] [9] were successfully applied. Further, research outcomes from vertical axis wind turbine studies are considered even though a straight transition to the VAT application

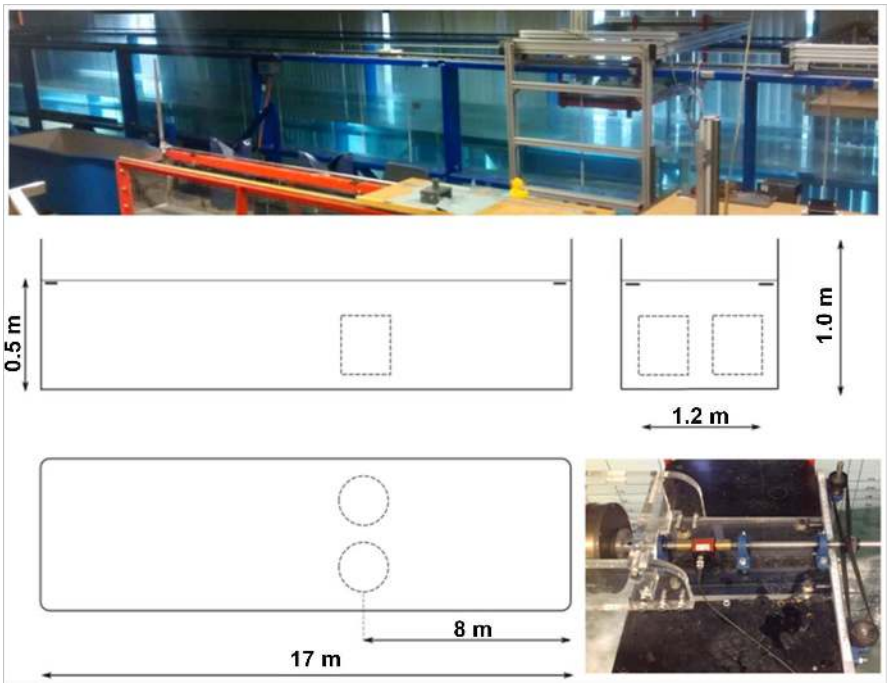

Figure 3. Laboratory flume at Cardiff University and main dimensions of the twin turbine system inside the flume. Bottom right: Power take off system composed of belts, main shaft, torque transducer and generator.

in water with its much higher density and lower flow velocities is not possible [10] [11] [12].

Considering outcomes from previous studies here in Cardiff [13] [14] [15], the most promising design parameters were chosen, experimentally tested, compared and analyzed. In the following, only the final design is described. Each rotor has a diameter of 360 mm and consists of: a 20 mm stainless steel shaft; two hubs to host the six spokes and three twisted blades of 300 mm height.

The performance of the rotor was assessed by quantifying its coefficient of performance (C_P) which is the comparison of the amount of energy available (P_a) and the amount of energy extracted (P_e) as shown in Equation (1).

$$C_P = P_e / P_a = (\tau * \omega) / (0.5 * \rho * A * v^3). \quad (1)$$

where τ is the measured torque, ω the rotational speed, ρ the density of water, A the rotors swept area and v the flow velocity. The rotor's performance is usually plotted as a function of its tip speed ratio (λ) which is defined as (2).

$$\lambda = (\omega * r) / v. \quad (2)$$

At a flow velocity of 1.09 m/s, the rotor achieved a C_P of up to 60% at a tip speed ratio of 1.9.

3.2. Twin Turbine Testing and Optimization

The aim of employing two rotors in a turbine system is to: 1) generate more than twice the amount of energy than a single rotor with the equivalent swept area, 2)

improve the self-starting behavior, 3) reduce torque fluctuations and 4) simplify the PTO (see Section 3.3). Li and Calisal suggested that the optimally configured twin system may benefit from an increased power output of 25% and a reduction of torque fluctuations. However, it was also noted that the highest performance setting may not coincide with the least torque fluctuations [16] [17].

In this study, the focus is on observing the best performing twin setup by optimizing the: 1) direction of rotation, 2) spacing between the rotors and 3) rotor synchronization. The blockage ratio β (turbine swept area over channel cross-section) was kept constant at 36%. Several studies such as [18] [19] have investigated the impact of blockage on performance and how to appreciate this issue. However, the researched turbine will operate in blocked conditions (in canals) and a potential blockage correction was therefore not applied.

1) Direction of rotation

The torque a blade generates during a revolution is not constant and peaks between 0˚ and 90˚ [20]. It was therefore decided to assemble the rotors counter rotating in such a way that their torque peak is towards the center of the channel where the velocities are expected to be the highest. Figure 4 depicts the experimental set-up and the results of testing the efficiency of the twin system while the rotors are counter-rotating (A) and co-rotating (B). It was shown that the efficiency for case A peaked at 78% and for case B at 75%. Further, the rotors spun slightly faster in case A.

2) Distance between rotors

Another parameter of interest is the optimum distance between the two rotors. Only symmetrical arrangements were considered with the centerline of the channel being the line of symmetry. Four different axis-to-axis spacings (1.4D, 1.5D, 1.6D and 1.75) were tested in order to determine the optimum spacing between the rotors. Figure 5 depicts the experimental set-up and data in terms of performance curves. For an axis-to-axis spacing of 1.5D, the turbine attained

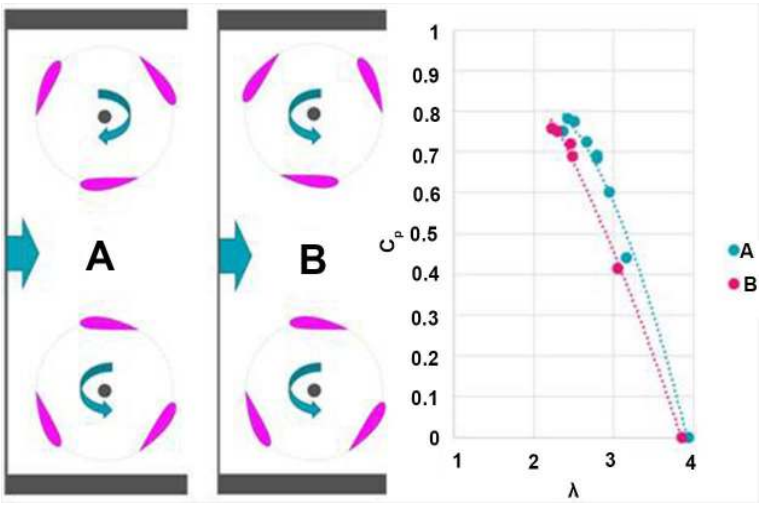

Figure 4. LHS, Sketch of experimental set-up. RHS, C_P vs λ for counter-rotating rotors (A) and co-rotating rotors (B) at v = 0.9 m/s.

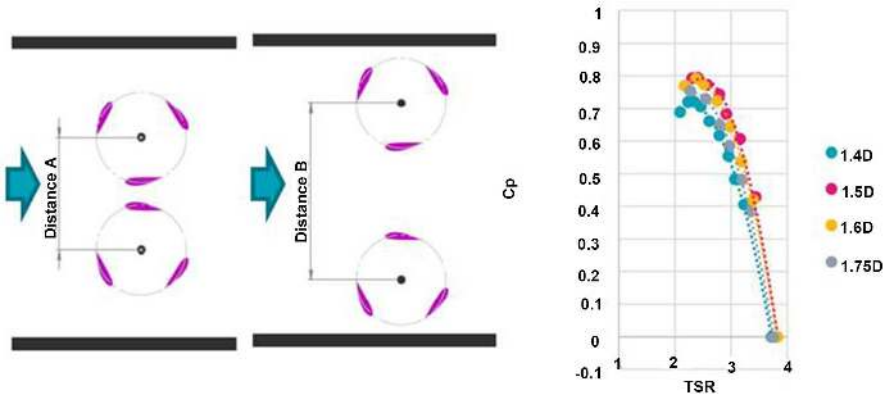

Figure 5. LHS, Sketch of experimental set-up. RHS, C_P vs λ for various distances between rotors at v = 0.9 m/s.

a C_P of 79% at a flow velocity of 0.9 m/s and 74% at a velocity of 1.09 m/s (not shown in the graph) which equates to an increase in efficiency of 23% compared to a single rotor at 1.09 m/s.

3) Rotor synchronization

The twin rotor design includes the concept of having just one PTO for both rotors by employing a timing-belt drive that transfers the torque of each rotor onto one common shaft (**Figure 2**). This saves using two separate PTO's and hence higher costs of investment. It was tested whether the combination of the motion and synchronization of the rotors (C) results in a disadvantageous performance compared to having both rotors spinning independently (A). The experimental set-up and results in terms of performance curves are shown in **Figure 6**. It was confirmed that both, rotational speed and performance in option C (λ = 2.1, C_P = 75%) lacked behind option A (λ = 2.5, C_P = 78%) which is due to the additional drag torque of the belt drive.

3.3. Closure

The twin turbine design (1:10 scale) was successfully tested in the laboratory and is ready for upscaling to a real canal environment. The very latest laboratory tests showed turbine coefficients of power of above 75%. Conclusions and recommendations from the laboratory tests are as follows:

Rotor: The hydrodynamic behavior of the rotor and its components is well understood and, as far as performance is concerned, the rotor operates very well above a C_P of 0.5. The current design, however, needs confirmation by upscaling and field testing.

Structure: Similar to the rotor, the hydrodynamics of the structure is well understood and the design can be applied for testing in real conditions. Besides improving the overall performance of the turbine, the key feature of the structure is to assemble the entire system in a safe and efficient way.

Twin turbine assembly: The twin turbine operates with high efficiencies in the laboratory and is ready for the application on site. The hypothesis that the

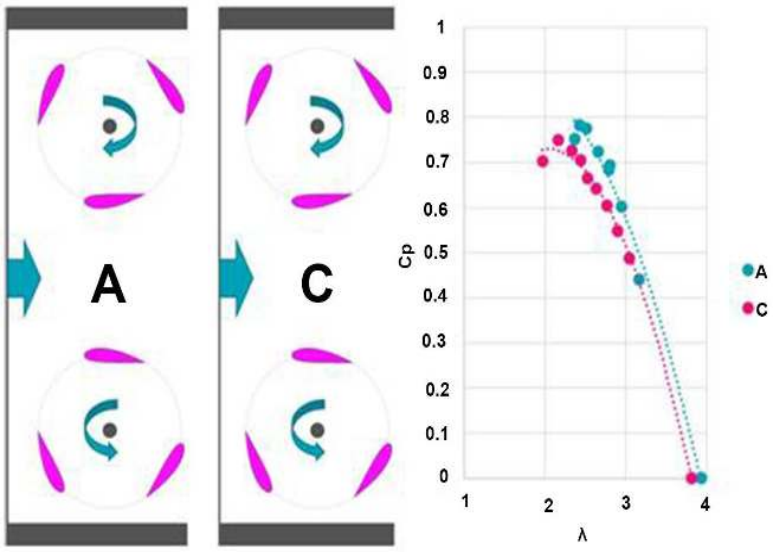

Figure 6. LHS, Sketch of experimental set-up. RHS, C_P vs λ for synchronized rotors (A) and independent rotors (C) at v = 0.9 m/s.

twin-turbine setup can provide additional efficiency compared to a single rotor was confirmed.

Drivetrain: In several laboratory experiments, the belt-drive has shown its potential for solving mechanical difficulties such as changing direction and orientation of an applied torque while ensuring a safe and continuous operation.

Power take-off: On the 11th of March 2016, the twin rotor could generate power for the first time by using a manually controlled low-speed three-phase AC generator instead of the breaking mechanism. Integrating the gearbox is planned for TRL 7, a functional power control and grid integration is planned for TRL 8.

The twin turbine shows a very promising performance and is ready for up-scaled field testing. At this stage the system reached TRL 5.

4. Hydrokinetic Twin Turbine Pilot Scale Testing (TRL 6)

The next step in the development of the system is to up-scale the turbine to a pilot/scale (1:3 scale) and demonstrate its successful operation in a relevant environment with the goal of achieving TRL 6.

An upscaled version of the laboratory-scale twin-rotor vertical axis turbine system was designed and deployed in a UV radiation channel, which is the last stage of water treatment at the RM Clayton water treatment plant, in Atlanta, Georgia. The deployed turbine consisted of two low solidity, three-bladed, counter-rotating rotors, a belt drive to combine the rotational motion and torque to one shaft and a power take-off (PTO) system. In order to increase the flow velocity and achieve maximum performance, a flow diversion structure was installed in the channel. In the following the steps from design to deployment are outlined and the test results in the form of power curves are reported.

4.1. Testing Environment and Turbine Design

Figure 7 sketches the UV channel into which the turbine was installed, including the clearance of the UV lamp (yellow circle), the flow diverter (orange) and the turbine consisting of a submerged twin rotor system and a PTO that is located above the channel. The channel is approximately 1.9 m wide and 4 m deep, and the inflowing water is controlled via a rectangular weir and a gate. The water flows at a depth of approximately 1.9 m through the UV-radiation lamps upstream of the turbine rotors. The flow diverter's function is to force the water to flow through a smaller cross-sectional area thereby increasing its velocity so that a reasonable amount of hydrokinetic energy was available for extraction. The water then drives the two counter-rotating rotors and consequently the main drive shaft that was positioned on a PTO bridge above the channel. Downstream of the rotors, the water discharges over a weir into a channel eventually releasing the treated water into the Chattahoochee River.

The main aim of the flow diverter is to reduce the cross sectional area of the channel with the aim to increase the flow velocity in the remaining cross-section. With a given discharge (Q), which varies throughout the day, the spatially-averaged flow velocity (V) in the channel is only a function of the cross-sectional area (A) and is obtained as:

$$V = Q/A \tag{3}$$

Therefore, the flow-velocity in the channel increases linearly with the reduction of the cross sectional area. Here, the area of the constriction (2.01 m^2) is a bit more than half of the area of the wetted channel cross sectional area (3.61 m^2) and therefore, reasonable flow velocities are expected in an otherwise relatively low-velocity channel.

The constriction, to be seen in Figure 7 and Figure 8, is shaped to minimize hydrodynamic losses in the form of dead zones or recirculation zones and to smoothly accelerate the water before approaching the rotors by maintaining its slope just below 30˚. The upstream extent of the constriction is limited by the UV lights clearance radius. The bottom shaft bearings are attached to the constriction.

The water depth in the UV channel is approximately 1.9 m, however the entire depth of the UV channel is approximately 4 m. The power-take-off (PTO) system is located on a bridge above the UV channel, hence, very long rotor shafts are required. In order to avoid extensive bending of the rotors' shafts, a middle bridge is introduced with two additional bearings attached to it. The bridge was installed close to the water surface to minimize bending of the shaft close to the rotors.

The upper bridge is depicted on the left hand side of Figure 8 and serves multiple purposes including supporting the top bearings of the rotor shafts, accommodating the PTO and covering the UV channel. It is designed in mild steel with a coating applied to prevent corrosion and is attached via bolts to the concrete.

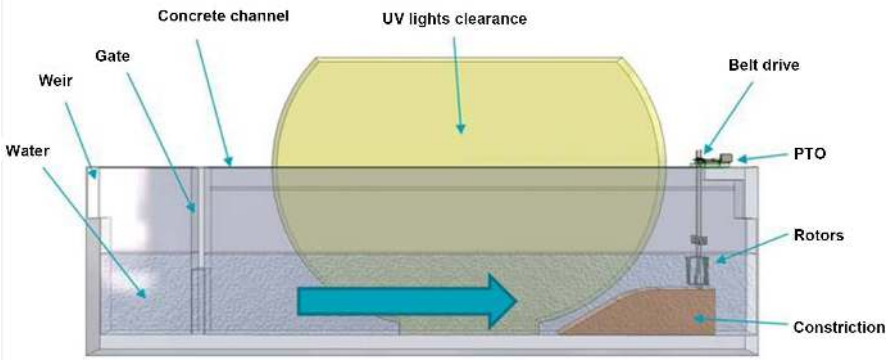

Figure 7. Side view of the UV channel at RM Clayton, Atlanta, including the various turbine components.

Figure 8. LHS, photograph of upper bridge as installed in RM Clayton including PTO and belt drive. RHS, photograph of downstream view of constriction, rotors and middle bridge.

Figure 9 shows one of the two twin-rotors in various views, in the form of CAD construction drawings, as 3D Solid works drawings and a photograph as manufactured. Three main components comprise the rotor: three blades, six spokes and two hubs. The parameters of the rotor design and the general dimensions of the rotors utilized here are driven by the geometry of the channel and the constriction design.

4.2. Testing Procedure and Results

The hydrokinetic twin turbine is placed in the second of five disinfection channels, the final treatment stage (UV radiation) before the water is discharged into the Chattahoochee River. It was assumed that the total amount of water is distributed evenly amongst each channel in operation. The water level was fairly constant and hence the flow velocity varies proportional to the discharge.

The PTO shaft hosts a torque transducer (Futek TRS605) which allows quantification of rotor generated torque τ and rotational speed ω. The system was tested with a disc break and a generator.

In order to quantify the performance of the turbine and compare it to the laboratory results, the same testing procedure was adopted as during the

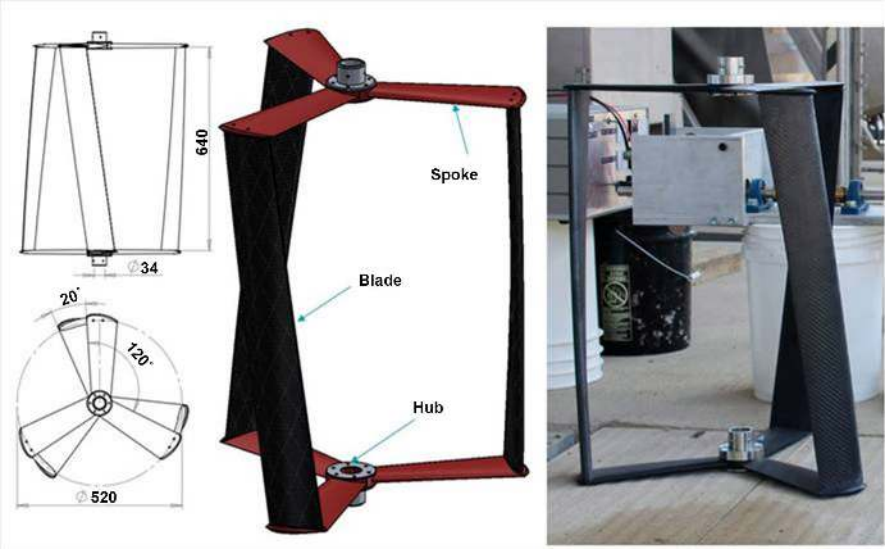

Figure 9. CAD drawings and photograph of the assembled turbine rotor.

laboratory tests as described before. In contrast to the laboratory flume, here, the discharge/velocity varied. The flow velocity was therefore measured by a propeller meter (Global Water FP211) and these measurements were compared with the cross-sectional velocity as computed via the discharge data provided by the plant operators and this is plotted in **Figure 10**.

Figure 11 presents turbine performance curves for three tests using the discharge data provided by the plant. It can be seen that a minimal change in flow velocity can have a significant impact on the coefficient of performance (the smaller the velocity the higher C_p) and also an impact on λ (the smaller the velocity the higher λ) since both variables are functions of the flow velocity.

It can further be seen that some measurement points (circles in **Figure 11**) do not follow the general trend of the curve. In case of test 160, a general trend is even difficult to observe. The curve for test 161 has an almost ideal shape. In the graph for test 162, the last two points are higher than expected. Here, it may be assumed that the discharge and, hence the velocity, has changed during testing, which is not surprising given the fact that the discharge in the treatment plant always varies during the day.

The given turbine design is expected to perform slightly worse than in the laboratory where the flow conditions are ideal and where maximum turbine efficiencies of more than 75% were achieved. In addition to the non-uniform flow conditions (due to the turbulence downstream of the UV lights and the flow acceleration from the diverter), the tested turbine employs three bearings due to the very long shaft and this introduces additional friction. Hence, the maximum coefficient of performance of test 162 is more likely around 70%. The TSR of slightly less than 3, as expected, again due to the friction from bearings and belts and hence the curve 162 appears to best represent the turbine's performance.

A second set of performance data was gathered by employing a low rpm permanent magnet generator instead of the disc brake. The electrical power output

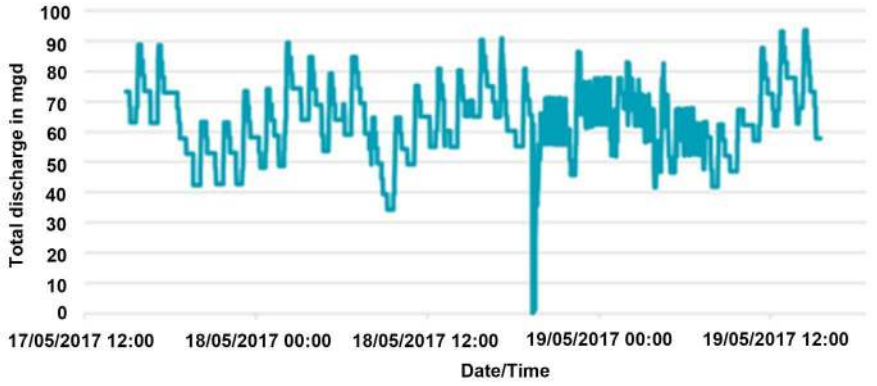

Figure 10. Discharge time history over testing period (17th May 2017 - 19th May 2017) as provided by the plant operator.

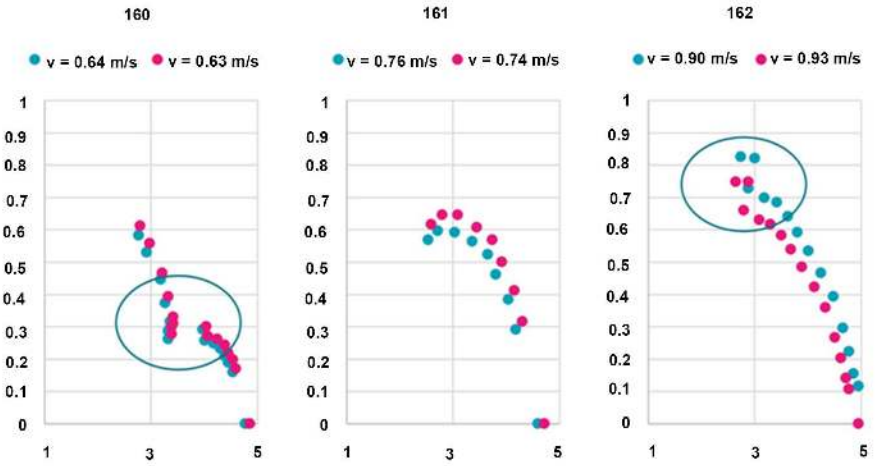

Figure 11. Test results with C_p on the y-axis, λ on the x-axis, measured (blue) and calculated (red) flow velocities (v).

in terms of voltage and current was measured using simultaneously two multimeters. At the same time, rotational speed and torque was measured and recorded analogously to previous tests. Instead of applying a disk brake the generator load was controlled using a resistor bank (see top right photograph of **Figure 12**) and the resistance was varied manually. Over a period of one minute per resistor setting, the voltage and current average readings were recorded together with torque transducer values. From these measurements mechanical power and electrical power were computed and provided in form of $C_p - \lambda$ curves in **Figure 13**. The achieved mechanical efficiency by considering a measured flow velocity of 0.9 m/s (blue, from the propeller meter) or a calculated velocity of 0.94 m/s (red, from the discharge data). There is some variation in the readings, again because the discharge was not constant over the testing period. The graph in the middle of **Figure 13** is a more realistic result of the performance here using 1 m/s velocity which was measured at the beginning of the test instead of the 0.9 m/s measured near the end of the test. The calculated power using measured data such as torque, rotational speed, voltage and current is plotted versus tip

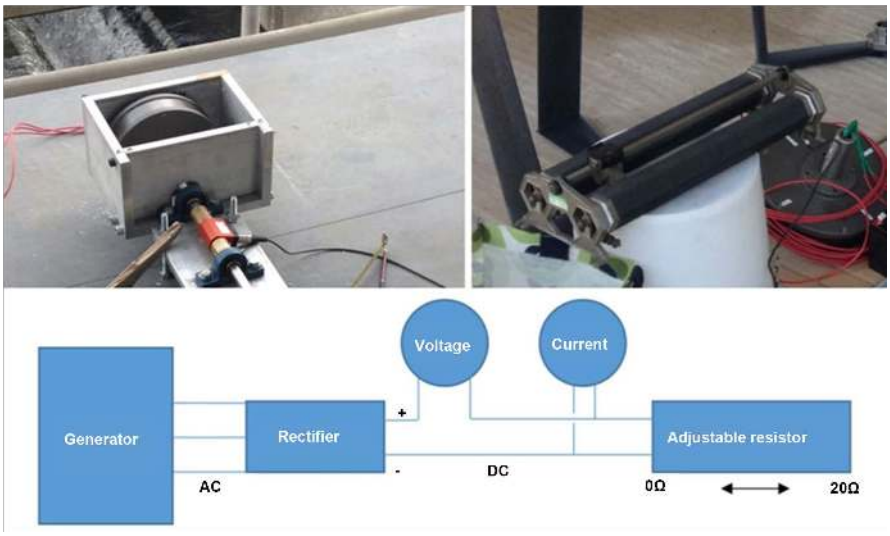

Figure 12. Top LHS, PTO including low RPM generator. Top RHS, adjustable resistor bank. Bottom, schematic of the electrical circuit for phase b and c testing.

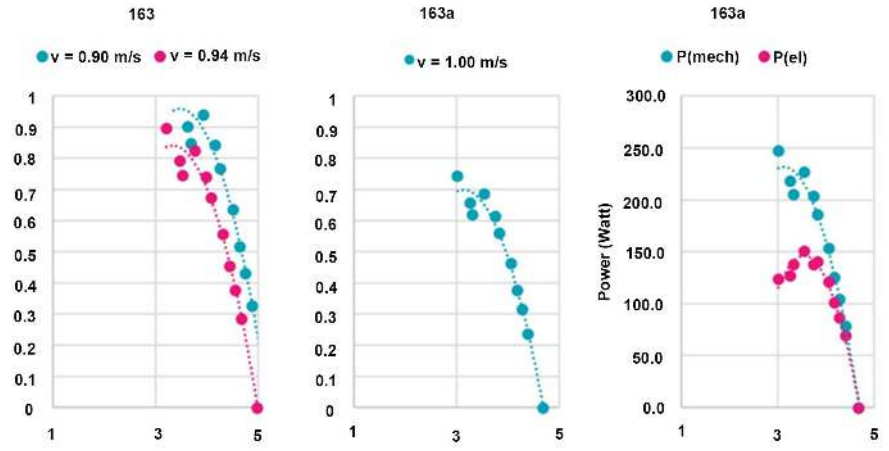

Figure 13. Performance curves with C_p on the y-axis (except RHS), λ on the x-axis, using measured (blue) and calculated (red) flow velocities (v) of test 163 (left). Same curve as before with a velocity of 1 m/s (probably more realistic and observed briefly at the beginning of the experiment) and power output in Watts from mechanical and electrical PTO as a function of λ (right).

speed ratio which is presented in the left curve in **Figure 13**. The difference between mechanical and electrical power output is very high, there are significant electrical losses from the generator (peak efficiency of 85%), the rectifier and the resistor bank in particular as it got very hot towards the peak performance. Further the generator is rated at 200 W at 200 rpm and the turbine is producing more energy at 200 rpm, *i.e.* approx. 230 W@200 rpm and hence the efficiency of the generator may be significantly lower than 85% which is also seen in the drop-off of the red curve near peak power.

4.3. Closure

The twin turbine design (1:3 scale) was successfully built, installed and tested at

a water treatment plant in Atlanta, and is ready for full scale application. The following conclusions and recommendations for future deployments from design to operation of the turbine can be summarized as follows:

Design: The turbine was designed based on successful laboratory tests carried out at Cardiff University. For the particular deployment site a flow diverter was designed to increase the flow velocity approaching the turbine in the otherwise very slow flowing UV channel. The rotor design included a very long stainless steel thick-walled tube in order to save weight.

Manufacturing: Except for the spokes, the rotor and PTO parts were manufactured at Cardiff University due to the availability of high-quality machining equipment and carbon fiber fabrication tools. A local contractor, manufactured most of the material for the two bridges and delivered it to the site. The spokes, casted out of glass-reinforced Nylon.

Installation: The installation was successfully led by a contractor with support from Emrgy. The installation took longer than expected mainly due to missing or not matching components. The reasons for these delays vary but in general it was observed that a more careful design (see note on shafts above) and preparation is necessary. In particular, it should be ensured that precision-machined/manufactured components such as shaft and bearings match perfectly prior to installation/deployment.

Testing: The test procedure was identical to the one used for the laboratory tests at Cardiff University. The routine was known and proven in more than 150 laboratory tests. The only uncertain quantity was the flow velocity due the varying effluent discharge. Initially, after installation, three channels were in operation and the discharge/flow velocities were very low (test 160, v = 0.64 m/s & 161, v = 0.76 m/s). After the plant manager closed one of the three channels the velocity increased to approximately v = 0.9 m/s. Due to the fact that the tests took place in a fully operating treatment plant, the discharge varied constantly and was never really constant over a typical total testing time of approximately half an hour. Hence, the quantification of the turbine's tip speed ratio (λ) and coefficient of performance (C_P) include some uncertainty. In order to minimize the uncertainty the measured approach flow velocity was cross checked with discharge data from the plant operator and found to vary within 5%. Mechanically, a maximum C_P value of around 70% for an operation at $\lambda = 3$ was achieved. Electrical tests were controlled manually via a resistor bank, in the future this aspect needs to be done automatically.

Operation: The turbine is currently in operation and has been equipped with a power take-off and control assembly which divert the generated power either to a battery or a dump load. The long-term operation of the turbine is important to gather information about wear and tear of individual components and to obtain as many operation hours as possible. Regular site visits are scheduled to observe the proper functioning of the system.

After successful testing and operation of the hydrokinetic twin turbine it can be concluded that the system has reached TRL 6.

5. System Commissioning (TRL 7)

The next step in the development stage of the turbine system is the deployment of an array of full-size turbines into the South Boulder Canal (SBC) near Denver. The South Boulder Canal is operated by Denver Water and it diverts water from Gross Reservoir into Ralston Reservoir. The canal is divided in three sections (A, B and C) and ten turbines are installed in all sections. The first turbine was deployed into Section A, see Figure 14, in June 2017, which is the last section of the SBC before the water enters the Ralston Reservoir via a "dragon's teeth" spillway structure. The section is approximately 30 m long and 5 m wide, of rectangular cross-section and the turbine was placed at the very end of section A. In the following, the rotor design, the testing procedure and the data analysis are documented.

5.1. Testing Environment and Turbine Design

The upper picture of Figure 15 depicts the turbine consisting of a concrete/steel structure, two rotors, a chain-drive-train (covered), a speed increaser gearbox and an asynchronous generator.

The rotors have a height of 0.8 meters and a diameter of 1.36 meters. The twin-rotors are counter-rotating, *i.e.* the right-hand-side rotor rotates clockwise and the left-hand-side rotor rotates anticlockwise. Each rotor shaft hosts a sprocket and the torque generated by the rotors is transmitted via a chain which drives the gearbox and eventually the generator. The focus of the tests reported here was on the mechanical power generated by the turbine and hence the electrical PTO was replaced by a mechanical PTO before deployment.

5.2. Procedure and Results

As described in the previous sections, the turbine's performance was tested by comparing the mechanical power at the main PTO shaft with the hydrokinetic energy available in the flowing water. The gearbox/generator assembly was replaced with a mechanical PTO that consists of a hydraulic disc break and a torque transducer. Figure 15 depicts the drivetrain and the mechanical PTO on the turbine housing while in operation in the SBC. The torque transducer was placed immediately before the disc break so that the measured torque and rotational speed included all losses of the rotor (mainly in the bearings) and the chain drive.

The flow rate Q in the SBC was provided by Denver Water and confirmed by measurements taken by the United States Bureau of Reclamation. The flow velocity was calculated by employing Equation (3) where A is the submerged cross-sectional area of the turbine housing at the position of the rotors. The estimation of A requires water level measurements just upstream and downstream of the housing and the average of the two readings was taken as the water depth.

The rotational speed and torque were recorded for one minute at a frequency of 200 Hz with a certain breaking force applied. The first 1 minute measurement

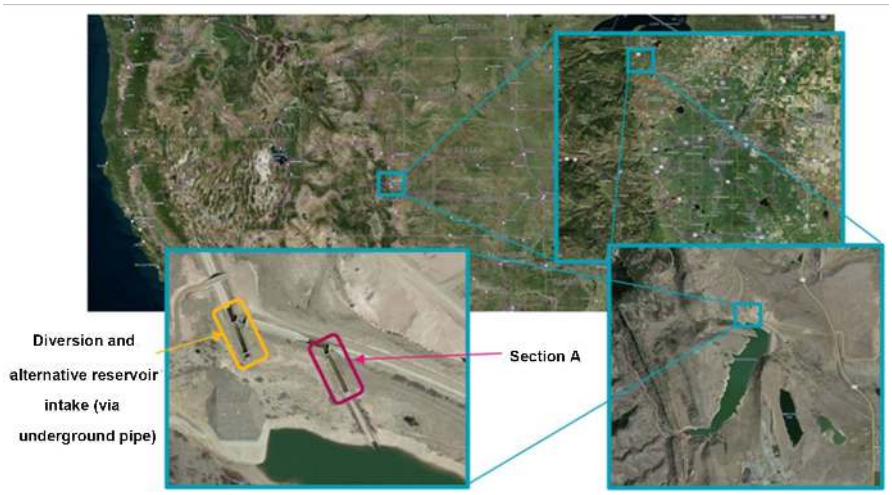

Figure 14. Satellite images depicting the location of section A of the South Boulder Canal at Ralston Reservoir near Denver, Colorado, US (source: Bing and Google Maps).

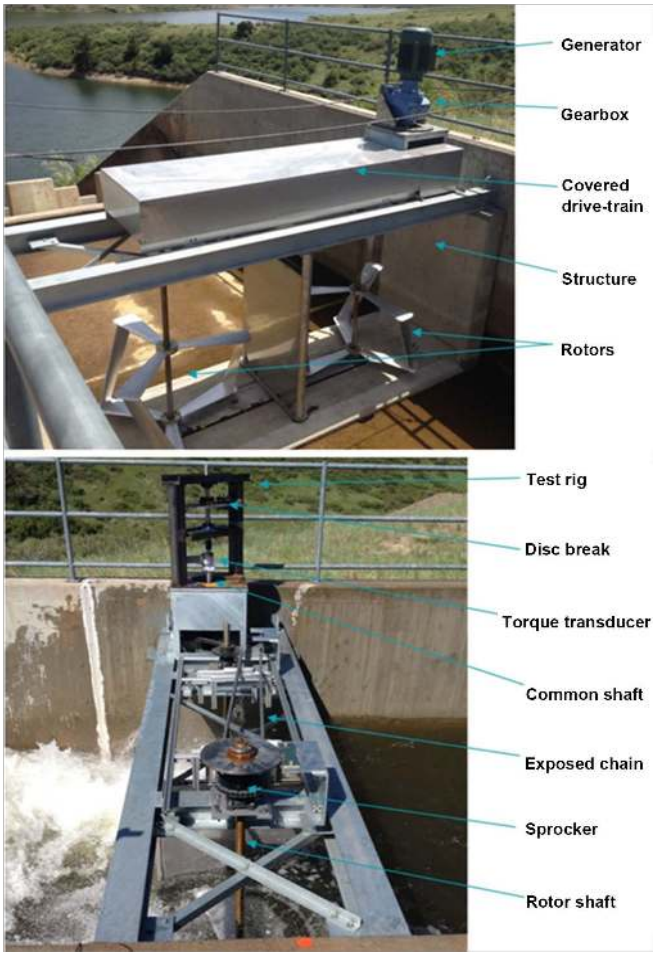

Figure 15. Emrgy's Hydrokinetic Twin Turbine and its main components during testing at Ralston Reservoir. Top, operational set-up including generator, gearbox and drive-train-cover. Bottom, test set-up including disc break, torque transducer/encoder and exposed chain drive.

period was conducted at free-wheeling of the rotors (*i.e.* no braking force applied) and the last 1 minute measurement was just before the turbine stalled, i.e. when the breaking force was maximum and the turbine stopped rotating. Five tests (Tests 165 to 168) were carried out and the results are summarized on the following pages.

The time-averaged raw data from the torque transducer (torque and rotational speed) and the computed mechanical power (including drive-train losses) for tests 165 to 168 are presented in Figure 16 in the form of the previously established turbine performance curves

For each of the five tests the efficiency of the turbine, *i.e.* comparing the measured turbine power with the available kinetic energy from the flowing water at the turbine housing's cross-section, is computed using Equation (1) and the tip speed ratio is calculated using Equation (2) and this is done for every 1 min measurement interval.

The discharge was provided by the channel operator Denver Water and was supposedly constant during the tests at Q = 250 cfs (7.08 m^3/s). Based on the average of measured upstream and downstream water depths (at the upstream and downstream side of the housing) the submerged cross-sectional area at the turbine shaft was calculated as A = 4.54 m^2. With the given constant discharge the flow velocity was computed as v = 1.56 m/s. During tests 167 and 169 it was observed that the water level dropped a little bit suggesting that the discharge was not constant, however no water level measurements were taken for these tests. It

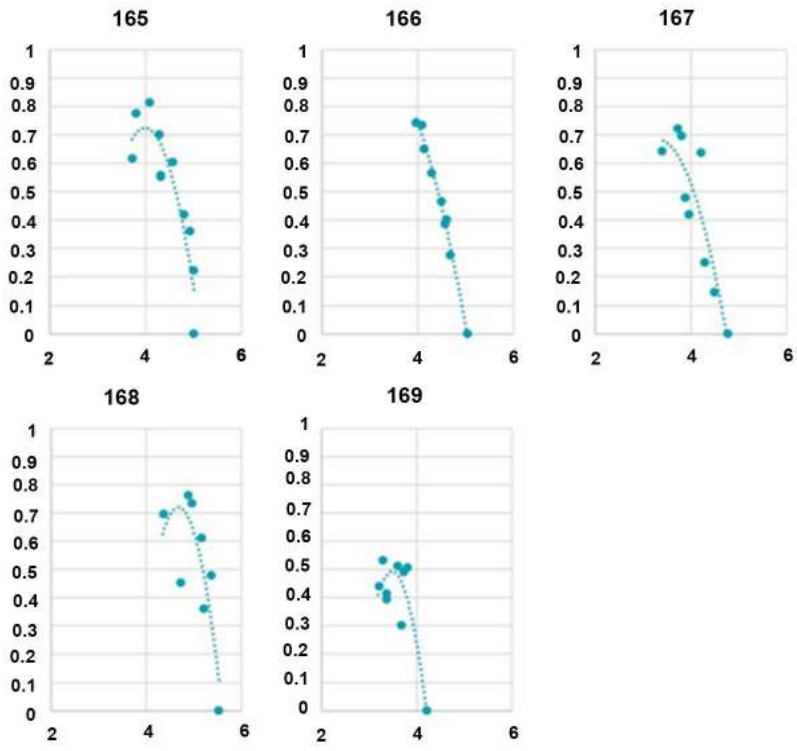

Figure 16. Turbine performance curves with C_p on the y-axis vs λ on the x-axis, for the five tests and based on flow velocity of v = 1.56 m/s.

was observed that the rotors were sometimes fully submerged (during Tests 168), and sometimes not (during Tests 165, 166, 167 and 169) and this has an impact on turbine performance. The turbine achieved peak efficiencies consistently above 70% during tests 165, 166, 167 and 168, whereas the peak efficiency of test 169 is only just above 50%. Also plotted are dashed trend lines (dashed lines) of the turbine-performance curve and as can be seen some data points clearly lie outside of the trend line (except during test 166), which reflects significant variation in the conditions that the turbine was operating in. The variation could be due to several factors, such as sudden discharge surges (increase, e.g. peaks around 80% during test 165, or decrease, very low C_p values during test 169) or strong turbulence which would result in sudden and local velocity spikes and/or drops.

A great effect on turbine performance has the submergence of the rotor, obviously if the rotor is fully submerged then the entire blade surface area is in contact with the water and therefore, more energy can be extracted in comparison with a rotor that is not fully submerged and for which not the entire blade area is in contact with the water. In addition, the blade-hydrodynamics are disturbed if the blades are not fully submerged, e.g. by air-entrainment which reduces the density of the water that is in contact with the blade, and hence, this results in a reduction of lift forces generated in this area. The exact decrease in performance of an emergent rotor has not been quantified, however, it was observed that during tests 165, 166, 167, 169 the top part of the rotor, mainly the upper spokes, were slicing through the water surface during their upstroke movement. This resulted in significant splashing and most likely in an additional drag torque on the rotor shaft, which reduced the turbine's efficiency. For tests 165 - 167 still quite high efficiencies, >70%, were achieved. The peak of the performance curve in Test 169 is only around 53%, for a discharge of 250 cfs and it seems that the discharge during this test was most likely a bit lower than 250 cfs. This is supported by Figure 17 which plots the extracted power on the y-axis as a function of measured rotational speed at peak performance. The blue circles

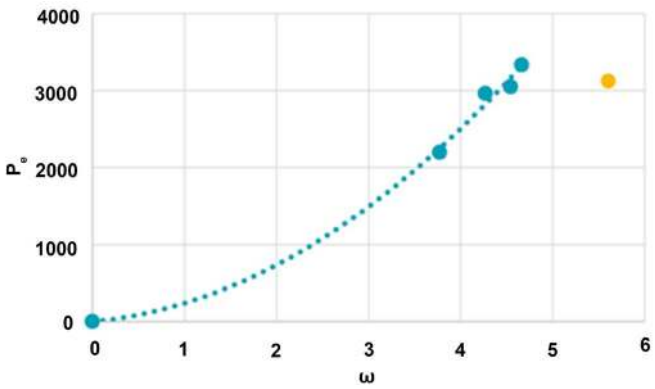

Figure 17. Turbine performance curve for all tests with extracted power P_e on the y-axis and rotational speed ω on the x-axis. Also added is a trend line through data points of tests 165, 166, 167, 169.

are tests 165, 166, 167 and 169 and they all fall very nicely on the dashed trend line. The lower data point is said test 169, and less discharge resulted in less rotational speed and less power produced. The yellow data point represents test 168, the only test where the rotor was fully submerged, but unfortunately during this test the discharge dropped suddenly and the test was aborted because the rotor was not fully submerged any more. The yellow data point clearly falls outside of the trend line: the rotational speed appears to be too high (point is too far to the left) for the power produced. Also, as can be seen from **Figure 16**, the TSR for the measured power was at approximately 5, which clearly suggests that the maximum power point was not yet reached at the moment the test was aborted. It remains to be seen whether a fully submerged rotor will be able to achieve even higher efficiencies than the ones achieved in tests 165, 166, 167, 169.

5.3. Closure

The hydrokinetic twin turbine was successfully built and deployed in the South Boulder Canal near Denver Water's Ralston Reservoir, Denver, Colorado, US.

During the tests, the turbine was subjected to a more or less constant flow rate of Q = 250cfs and mechanical torque and rotational speed were measured at the main shaft of the turbine while different loads were applied using a hydraulic disc-break. The turbine achieved a coefficient of performance consistently above 70% and was operating at a TSR of up to 4 for most of the tests. During peak performance up to 3.4 kW of mechanical power (including drive-train losses) was generated.

However, significant variation in the outputs was observed, during one of the tests the turbine appeared to underperform, and the coefficient of power was only about 50%. Detailed analysis of the measured torque and speed data suggested that the discharge must have decreased below the given 250 cfs. The tests revealed that rotor submergence is a critical factor in the operation of the turbine. An emergent rotor suffers from the additional drag torque when the rotor arms are slicing through the water surface and blade hydrodynamics is compromised when air is entrained. The turbine tests however highlighted that the turbine's efficiency remains high despite rotor non-submergence and it appears that the turbine housing, which provides local accelerations and thus high velocities that the rotor blades are exploiting during the rotor's upstroke, has a positive influence on turbine performance. The tests suggest that a fully submerged rotor operating in a turbine housing might be able to achieve efficiencies above 80%.

Finally, the scalability of the turbine was confirmed, the full-scale turbine at Denver operated similarly, if not better, than its smaller-scale versions tested in the laboratory and in Atlanta. It can be concluded that the twin turbine has successfully reached TRL 7.

6. Scalability

The purpose of using dimensionless quantities for the turbine performance

curve is to be able to demonstrate the scalability of the system, in other words, to be able to predict the turbine's performance irrespective of its size. Figure 18 presents three turbine performance curves obtained under different conditions and for three turbines of different size, *i.e.* the 1:10-scale lab turbine, the 1:3-scale turbine deployed at RM Clayton, Atlanta and the full-scale turbine deployed in the South Boulder Canal near Denver, CO. Due to the fact that each turbine has a slightly different rotor solidity the tip speed ratio, TSR, was multiplied with the solidity to account for the fact that the rotational speed is directly affected by the solidity of the rotor. The rotor spins faster at lower solidity and slower at higher solidity.

First of all, it seems that the three curves are very similar and peak efficiencies are around 70%. Secondly, the rotational speeds (times solidity) at free-wheeling are very similar for the Atlanta and laboratory turbines, whereas the Denver turbine appears to rotate slower than the other two. This is probably due to the effect of non-submergence and aforementioned drag torque created when the arms slice through the water. In contrast, the Denver turbine appears to yet feature a greater peak efficiency and this is most likely because the Denver turbine operated in a housing whereas the other two turbines did not. Apparently, the Denver turbine benefitted from the additional flow acceleration caused near the housing's sidewalls on the upstroke of the rotor. The effect of the housing on the turbine performance could not have been quantified in the laboratory and in Atlanta due to the limited width of the flume or channel, respectively.

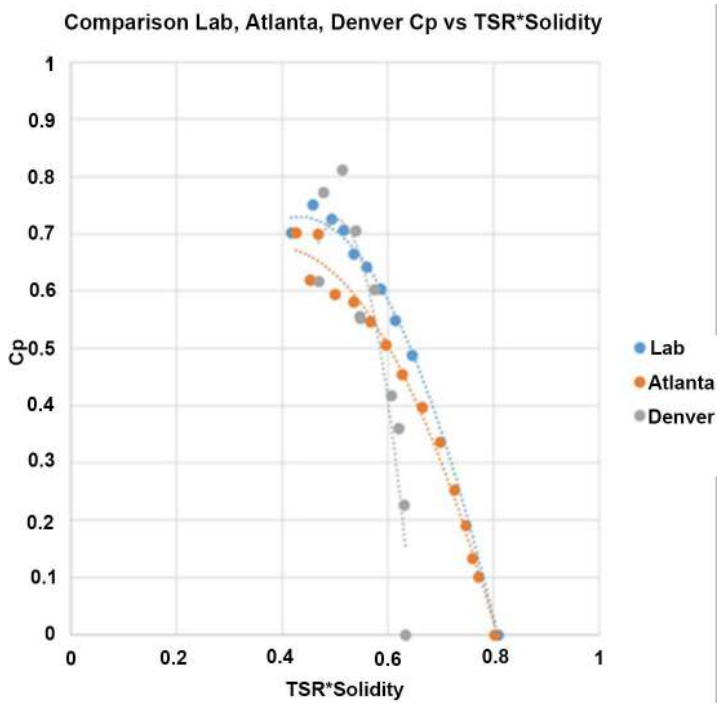

Figure 18. Performance curves of three selected tests, Laboratory, Atlanta and Denver of the turbine operating in different environments and at different size.

7. Conclusions

It is concluded that the previously described hydrokinetic twin turbine for harvesting energy from flowing water in man-made channels successfully reached TRL 7 (Full-scale, similar (prototypical) system demonstrated in relevant environment).

The development started with a concept (TRL 1 - 3) of a counter-rotating, vertical-axis twin turbine embedded in a hydrodynamic beneficial housing to be deployed in man-made channels.

Over a period of two years, a 1:10-scale model of the turbine was built and tested in the laboratory at Cardiff University. The laboratory tests concluded that turbine efficiencies of more than 75% could be attained. The turbine had reached TRL 5 (laboratory scale, similar system validation in relevant environment) and was ready for upscaling and testing in a real channel environment.

In May 2017, a 1:3-scale turbine system was installed into a UV radiation channel, the last stage of water treatment at the RM Clayton water treatment plant in Atlanta, GA. The twin turbine was successfully built, installed and tested and is still in operation in order to supply an electronic display board and thereby reached TRL 6, which is considered an engineering/pilot-scale, similar (prototypical) system validation in relevant environment. The turbine was thus deemed ready for full-scale application.

Later in 2017, the turbine system was deployed as an array of ten full-size turbines (Emrgy's Hydrokinetic Twin Turbine) into the South Boulder Canal (SBC) near Denver. The system was tested and compared to the previous development stages and the scalability of the design was confirmed as well as the functionality and the excellent performance. All design components such as housing, drive-train, gear-box and generator were tested and operational and thus TRL 7 was achieved.

Acknowledgements

This research has been supported by EPSRC (1611593) and Emrgy Inc., Atlanta, GA, which is gratefully acknowledged.

Conflicts of Interest

The authors declare no conflicts of interest regarding the publication of this paper.

References

[1] Güney, M.S. and Kaygusuz, K. (2010) Hydrokinetic Energy Conversion Systems: A Technology Status Review. *Renewable and Sustainable Energy Reviews*, **14**, 2996-3004. https://doi.org/10.1016/j.rser.2010.06.016

[2] Güney, M.S. (2011) Evaluation and Measures to Increase Performance Coefficient of Hydrokinetic Turbines. *Renewable and Sustainable Energy Reviews*, **15**, 3669-3675. https://doi.org/10.1016/j.rser.2011.07.009

[3] U.S. Department of Energy, Technology Readiness Assessment Guide, DOE G

413.3-4A. (2015)
https://www.directives.doe.gov/directives-documents/400-series/0413.3-EGuide-04-admchg1/@@images/file

[4] Stoesser, T., Morris, T., Morris, E., Walsh, A., Vanselous, J., Parys, C.L. and Tutas, B.D. (2017) Turbine Hydrokinetic Energy System Utilizing Cycloidal Magnetic Gears. Patent No. WO 2017172747.

[5] Shiono, M., Suzuki, K. and Kiho, S. (2000) An Experimental Study of the Characteristics of a Darrieus Turbine for Tidal Power Generation. *Electrical Engineering in Japan*, **132**, 38-47.

[6] Ouro, P., Stoesser, T. and McSherry, R. (2015) Large-Eddy Simulation of a Vertical Axis Tidal Turbine Using an Immersed Boundary Method. Chapter 5, CFD for Wind and Tidal Offshore Turbines, Springer, 49-58.

[7] Li, C., Zhua, S., Xu, Y.L. and Xiao, Y. (2013) 2.5D Large Eddy Simulation of Vertical Axis Wind Turbine in Consideration of High Angle of Attack Flow. *Journal of Renewable Energy*, **51**, 317-330. https://doi.org/10.1016/j.renene.2012.09.011

[8] McNaughton, J., Billard, F. and Revell, A. (2014) Turbulence Modelling of Low Reynolds Number Flow Effects around a Vertical Axis Turbine at a Range of Tip-Speed Ratios. *Journal of Fluids and Structures*, **47**, 124-138. https://doi.org/10.1016/j.jfluidstructs.2013.12.014

[9] Maitre, T., Amet, E., Pellone, C., Lee, Y. and Kim, S. (2013) Modeling of the Flow in a Darrieus Water Turbine: Wall Grid Refinement Analysis and Comparison with Experiments. *Journal of Renewable Energy*, **57**, 497-512. https://doi.org/10.1016/j.renene.2012.09.030

[10] Batista, N., Melicio, R., Matias, J. and Catalao, J. (2011) New Blade Profile for Darrieus Wind Turbines Capable to Self-Start. *IET Conference on Renewable Power Generation CRPG*, Edinburgh, UK, 6-8 September 2011, 1-5.

[11] Hwang, I., Min, S., Jeong, I., Lee, Y. and Kim, S. (2006) Efficiency Improvement of a New Vertical Axis Wind Turbine by Individual Active Control of Blade Motion. *SPIE Smart Structures and Materials + Nondestructive Evaluation and Health Monitoring*, San Diego, Vol. 6172, 8 p. https://doi.org/10.1117/12.658935

[12] Paraschivoiu, I., Trifu, O. and Saeed, F. (2009) H-Darrieus Wind Turbine with Blade Pitch Control. *International Journal of Rotating Machinery*, **2009**, Article ID: 505343. https://doi.org/10.1155/2009/505343

[13] Priegue, L., Stoesser, T. and Runge, S. (2015) Effect of Blade Parameters on the Performance of a Cross-Flow Turbine. *E-Proceedings of the* 36*th IAHR World Congress*, The Hague.

[14] Priegue, L. and Stoesser, T. (2017) The Influence of Blade Roughness on the Performance of a Vertical Axis Tidal Turbine. *International Journal of Marine Energy*, **17**, 136-146. https://doi.org/10.1016/j.ijome.2017.01.009

[15] Harries, T., Kwan, A., Brammer, J. and Falconer, R. (2016) Physical Testing of Performance Characteristics of a Novel Drag-Driven Vertical Axis Tidal Stream Turbine; with Comparisons to a Conventional Savonius. *Journal of Marine Energy*, **14**, 215-228.

[16] Li, Y. and Calısal, S.M. (2010) Modeling of Twin-Turbine Systems with Vertical Axis Tidal Current Turbines: Part I Power Output. *Ocean Engineering*, **37**, 627-637. https://doi.org/10.1016/j.oceaneng.2010.01.006

[17] Li, Y. and Calısal, S.M. (2011) Modeling of Twin-Turbine Systems with Vertical Axis Tidal Current Turbine: Part II Torque Fluctuation. *Ocean Engineering*, **38**,

550-558. https://doi.org/10.1016/j.oceaneng.2010.11.025

[18] Kinsey, T. and Dumas, G. (2017) Impact of Channel Blockage on the Performance of Axial and Cross-Flow Hydrokinetic Turbines. *Renewable Energy*, **103**, 239-254. https://doi.org/10.1016/j.renene.2016.11.021

[19] Schluntz, J.R. and Willden, H.J. (2015) The Effect of Blockage on Tidal Turbine Rotor Design and Performance. *Renewable Energy*, **81**, 432-441. https://doi.org/10.1016/j.renene.2015.02.050

[20] Islam, M., Ting, D.S.K. and Fartaj, A. (2008) Aerodynamic Models for Darrieus-Type Straight-Bladed Vertical Axis Wind Turbines. *Renewable and Sustainable Energy Reviews*, **12**, 1087-1109. https://doi.org/10.1016/j.rser.2006.10.023